TOXICOLOGICAL SCIENCES **115(2)**, 401–411 (2010)
doi:10.1093/toxsci/kfq070
Advance Access publication March 4, 2010

Integration of Mutation and Chromosomal Damage Endpoints into 28-Day Repeat Dose Toxicology Studies

Stephen D. Dertinger,*[,1] Souk Phonethepswath,* Dean Franklin,* Pamela Weller,* Dorothea K. Torous,* Steven M. Bryce,* Svetlana Avlasevich,* Jeffrey C. Bemis,* Ollivier Hyrien,† James Palis,‡ and James T. MacGregor§

*Litron Laboratories, Rochester, New York; †Department of Biostatistics and Computational Biology and; ‡Department of Pediatrics, University of Rochester Medical Center, Rochester, New York; and §Toxicology Consulting Services, Arnold, Maryland

[1] To whom correspondence should be addressed at Litron Laboratories, 200 Canal View Boulevard, Rochester, NY 14623. Fax: (585) 442-0934. E-mail: sdertinger@litronlabs.com.

Received January 11, 2010; accepted February 19, 2010

Two endpoints of genetic toxicity, mutation at the X-linked *Pig-a* gene and chromosomal damage in the form of micronucleated reticulocytes (MN-RETs), were evaluated in blood samples obtained from 28-day repeat-dosing studies typical of those employed in toxicity evaluations. Male Wistar Han rats were treated at 24-h intervals on days 1 through 28 with one of five prototypical genotoxicants: N-ethyl-N-nitrosourea, 7,12-dimethyl-12-benz[*a*]anthracene, 4-nitroquinoline-1-oxide (4NQO), benzo(*a*)-pyrene, and N-methyl-N-nitrosourea. Flow cytometric scoring of CD59-negative erythrocytes (indicative of glycosylphosphatidylinositol anchor deficiency and hence *Pig-a* mutation) was performed using blood specimens obtained on days −1, 15, 29, and 56. Blood specimens collected on days 4 and 29 were evaluated for MN-RET frequency using flow cytometry–based MicroFlow Kits. With the exception of 4NQO, each chemical induced significant increases in the frequency of MN-RETs on days 4 and 29. All five agents increased the frequency of mutant phenotype (CD59 negative) reticulocytes (RETs) and erythrocytes. Mutation responses in RETs occurred earlier than in erythrocytes and tended to peak, or nearly peak, at day 29. In contrast, the mutant phenotype erythrocyte responses were modest on day 29 and required additional time to reach their maximal value. The observed kinetics were expected based on the known turnover of RETs and erythrocytes. The data show that RETs can serve as an appropriate indicator cell population for 28-day studies. Collectively, these data suggest that blood-based genotoxicity endpoints can be effectively incorporated into routine toxicology studies, a strategy that would reduce animal usage while providing valuable genetic toxicity information within the context of other toxicological endpoints.

Key Words: **mutation; *Pig-a* gene; CD59; flow cytometry; genotoxicity; micronuclei.**

Integration of genotoxicity endpoints into repeat-dosing toxicity studies has several potential benefits. In addition to reducing the number of animals needed for safety assessment purposes, the genotoxicity results are expected to be more informative and interpretable when obtained in the context of general toxicology, metabolic, and pharmacokinetic studies (Blakey *et al.*, 2008; Hamada *et al.*, 2001; Krishna *et al.*, 1998).

While integration of genotoxicity endpoints is clearly attractive, and is encouraged in a number of guidance documents and other reports (International Conference on Harmonization, 2008; Pfuhler *et al.*, 2009; Center for Drug Evaluation and Research, U.S. Food and Drug Administration, 2006), practical obstacles to implementation exist. These are most pronounced in the case of assessment of gene mutation. Although transgenic animal models exist that allow measurement of mutant cell frequencies in virtually any tissue, their requirement for nonstandard rodent strains has hindered utilization of these systems for integrated studies. The endogenous *Hprt* gene mutation assay can be performed with standard laboratory animals, but its resource-intensive nature and limitation to tissues amenable to *in vitro* cell culture are significant barriers to widespread adoption.

This laboratory has previously described automated approaches for determining *in vivo* mutation frequencies at the endogenous *Pig-a* gene locus that overcome many of these practical issues (Bryce *et al.*, 2008, Phonethepswath *et al.*, 2008, 2010). This system utilizes flow cytometry to quantify mutant cells based on the glycosylphosphatidylinositol (GPI) anchor–deficient phenotype, a strategy first proposed by Luzzatto and colleagues (Araten *et al.*, 1999). Our proof-of-principle experiments have focused on identification of mutant phenotype erythrocytes in mouse and rat blood specimens. Dobrovolsky *et al.* (2010) and Miura *et al.* (2008a,b) have successfully applied similar flow cytometric scoring strategies to the analysis of mutant phenotype rat erythrocytes and splenic lymphocytes.

Recently, we described the kinetics by which mutant phenotype rat erythrocytes (i.e., CD59 negative, abbreviated RBC^{CD59-}) and mutant phenotype reticulocytes (RETs) (i.e.,

TABLE 1
Chemicals

Chemical	CAS no., purity	Vehicle	Dose levels (mg/kg/day)	Maximum tolerated dose reached?
ENU	759-73-9, 68% (high stabilizer content)	PBS, pH 6	2.5, 5, 10	Approached; reduced weight gain; severe reduction to % RET at 20 mg/kg/day in range finder
MNU	684-93-5, 75% (high stabilizer content)	PBS, pH 6	2.5, 5, 10	Yes; reduced weight gain; severe weight loss at 15 mg/kg/day in range finder
DMBA	57-97-6, $\geq$ 95%	Sesame oil	2.5, 5, 10	Yes; reduced weight gain; severe reduction to % RETs; morbidity and death observed on days 30–31
B(*a*)P	50-32-8, $\geq$ 96%	Sesame oil	37.5, 75, 150	Yes; reduced weight gain; severe weight loss at 200 mg/kg/day in range finder
4NQO	56-57-5, $\geq$ 99%	0.5% Methylcellulose in dH_2O	1.25, 2.5, 5	Yes; reduced weight gain; severe weight loss at 10 mg/kg/day in range finder; death in top dose group day 30

CD59 negative, abbreviated RET^{CD59-}) enter and are eliminated from the circulation after exposure to prototypical mutagens (Phonethepswath *et al*., 2010). These data indicated that mutant phenotype RETs and erythrocytes induced by some agents persist in peripheral blood for considerable periods of time, demonstrating that uncommitted hematopoietic stem/progenitor cells can continue to produce GPI anchor–deficient cells for at least 6 months. Those characteristics suggested that the assay would be highly compatible with subchronic and chronic toxicity studies, as mutants should accumulate with repeated dosing. Therefore, one objective of the current studies was to evaluate the sensitivity of the *Pig-a* assay in the context of the commonly conducted 28-day repeat-dosing study design.

A second objective was to assess the sensitivity of the rat peripheral blood micronucleated RET (MN-RET) endpoint in the context of a 28-day treatment schedule. Several published reports support the concept that this endpoint of cytogenetic damage can be integrated into routine toxicology studies (Hamada *et al*., 2001; MacGregor *et al*., 2006). However, as reflected by language that appears in the proposed International Conference on Harmonization Guidance on Genotoxicity Testing and Data Interpretation for Pharmaceuticals Intended for Human Use S2(R1) (2008), some concerns persist over the sensitivity of the assay when exposures occur at relatively low-dose levels for protracted periods of time (as compared to short-term acute studies using higher exposure levels). Data presented herein are discussed with this concern in mind.

MATERIALS AND METHODS

Reagents

Sesame oil, N-ethyl-N-nitrosourea (ENU; CAS no. 759-73-9), 7,12-dimethyl-1,2-benz[*a*]anthracene (DMBA; CAS no. 57-97-6), benzo(*a*)pyrene (B(*a*)P; CAS no. 50-32-8), 4-nitroquinoline 1-oxide (4NQO; CAS no. 56-57-5), and methylcellulose (CAS no. 9004-67-5) were purchased from Sigma-Aldrich, St Louis, MO. N-methyl-N-nitrosourea (MNU; CAS no. 684-93-5) was from Pfaltz & Bauer, Waterbury, CT. PBS (phenol red and divalent cation free) was from Mediatech, Inc., Herndon, VA. Heparin solution and all reagents necessary to perform the micronucleus analyses as described herein were from *In Vivo* Rat MicroFlow PLUS Kits (v090203, Litron Laboratories, Rochester, NY). Lympholyte-Mammal cell separation reagent was purchased from CedarLane, Burlington, NC (CAT no. CL5110). Anti-rat CD59, clone TH9, was custom-conjugated to phycoerythrin by BD Biosciences, San Jose, CA. SYTO 13 was purchased from Invitrogen, Carlsbad, CA (CAT no. S-7575). Proaerolysin was purchased from the University of Saskatchewan, Saskatoon, Canada.

Studies with Aerolysin

Experiments were performed to test the assumption that the CD59-negative phenotype is a reliable indicator of GPI anchor deficiency. These experiments utilized the toxin aerolysin, a high-affinity GPI anchor ligand that causes cell lysis (Diep *et al*., 1998). In one representative experiment, 7- to 8-week-old male Wistar rats were treated with ENU on three consecutive days via oral gavage (40 mg/kg/day). Three weeks after the final administration, blood was collected, leukodepleted, and stained for *Pig-a* analysis as described below. The numbers of CD59-positive and CD59-negative erythrocytes collected over a 6-min data acquisition period were recorded (i.e., time zero values). This same stained blood specimen was exposed to 0.75 μg aerolysin and incubated at 37°C. At 30-min intervals, the numbers of CD59-positive and CD59-negative erythrocytes were determined for 6-min data acquisition periods. These values were converted to a percentage of the time zero measurements. Note that just before use, proaerolysin was converted to aerolysin with trypsin according to manufacturer's recommendations.

Animals, Treatments, and Blood Collection

Experiments were conducted with the oversight of the University of Rochester's Institutional Animal Care and Use Committee. Male Wistar Han rats were purchased from Charles River Laboratories, Wilmington, MA. Rodents were allowed to acclimate for ~1 week before treatment. Water and food were available *ad libitum* throughout the acclimation and experimental periods. For the 28-day studies, each treatment group consisted of five randomly selected rats, age 7–8 weeks at the start of treatment, and each experiment included a concurrent vehicle control group. All treatments were via oral gavage in a volume of 10 ml/kg body weight. Test articles were administered at intervals of ~24 h on 28 consecutive days (days 1–28). Dose levels, vehicles employed, and other information are summarized in Table 1.

Blood specimens were collected from each animal on days −1, 15, 29, and 56. The samples obtained on day 29 (24 h after the last administration) are particularly important because this is the usual day of termination of 28-day

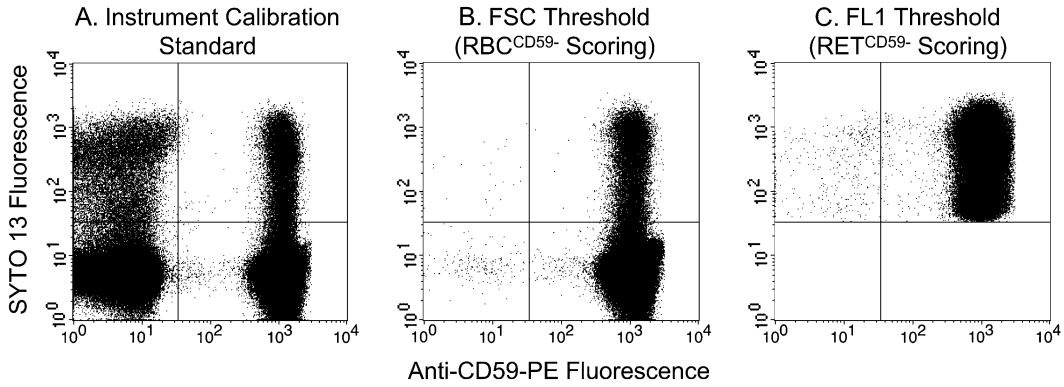

FIG. 1. Gated events (erythrocytes) are plotted on SYTO 13 versus anti-CD59-PE bivariate plots. Panel A: Instrument calibration standard; mutant-mimicking cells have been spiked into blood that were processed according to the standard protocol. This specimen provides enough events with a full range of fluorescence intensities to optimize photomultiplier tube voltages and compensation settings. This calibration standard also represents a means for rationally and consistently setting the position of the vertical line that defines mutant phenotype (CD59 negative) versus wild-type (CD59 positive) cells. Panel B: Day 29 blood specimen from a representative ENU-treated rat (10 mg/kg/day); by thresholding on the forward scatter (FSC) parameter, it is possible to efficiently evaluate 10^6 erythrocytes for the CD59-negative phenotype. Panel C: Day 29 blood specimen from the same ENU-treated rat shown in (panel B); by thresholding on SYTO-associated fluorescence (FL1), it is possible to efficiently evaluate 3×10^5 or more RETs for the CD59-negative phenotype.

toxicity studies. The significance of day 56 blood specimens (4 weeks after the last administration) is related to the fact that recovery animals are often included in 28-day studies, and the in-life portion is usually terminated between 2 and 4 weeks after the last treatment. Blood was obtained by nicking a lateral tail vein with a surgical blade after animals were warmed briefly under a heat lamp. Approximately 50–100 µl of free-flowing blood were collected directly into heparinized capillary tubes (Fisher Scientific, CAT no. 22-260-950). Immediately upon collection, 30 µl of each blood specimen were transferred to tubes containing 100 µl heparin solution (500 units/ml PBS) where they remained at room temperature for less than 2 h, after which time they were either immediately leukodepleted as described below or stored at 4°C until leukodepletion (within 1 h).

Cell Staining: Pig-a

The blood processing steps for *Pig-a* mutation scoring have been described in detail elsewhere (Phonethepswath *et al*., 2010). Briefly, each whole-blood/heparin specimen was leukodepleted with Lympholyte solution. At this stage, the resulting erythrocyte-enriched samples were immediately transferred to tubes that contained saturating phycoerythrin (PE) conjugated anti-CD59 or else stored at 4°C for later ($\leq$ 24 h) staining and analysis. After removing unbound antibody through centrifugation, cells were resuspended with 1 ml working nucleic acid dye solution (SYTO 13). After incubating for 30 min at 37°C, samples were placed on ice until flow cytometric analysis (within ~2 h).

Instrument Calibration Standard: Pig-a

On each day of analysis, an instrument calibration standard was prepared by creating a specimen with ~50% wild-type cells and 50% mutant-mimicking cells. The procedure for generating this specimen has been described previously (Phonethepswath *et al*., 2010). The resulting instrument calibration standard provided sufficient numbers of red blood cells (RBCs) that exhibited a full range of PE and SYTO 13 fluorescence intensities that were useful for optimizing photomultiplier tube voltages and fluorescence compensation settings on a daily basis. The position of the CD59-negative cells also provided a rational approach for defining the vertical demarcation line used to distinguish mutant cells from wild-type cells. See Figure 1, panel A.

Data Acquisition: Pig-a

A FACSCalibur flow cytometer (BD Biosciences) providing 488-nm excitation and running CellQuest Pro v5.2 software were used for data acquisition. For determination of the frequency of RBC^{CD59-} cells, data acquisition was triggered on the forward scatter parameter and the fluidics rate was set to low. See Figure 1, panel B. This facilitated efficient collection of 1×10^6 RBCs per specimen ($\leq$ 5 min). As these forward scatter–triggered analyses acquired 1×10^6 RBCs per specimen, they also provided a means to determine the frequency of RETs among total RBCs.

For determination of the frequency of RET^{CD59-}, the fluidics rate was set to medium and the data acquisition trigger was set on SYTO 13–associated fluorescence. This SYTO 13 threshold value was set sufficiently high such that the majority of RBCs (i.e., mature erythrocytes that lack RNA) were eliminated from consideration. See Figure 1, panel C. This strategy reduced file sizes and also allowed for a greater flow rate, making it possible to evaluate between 0.3 and 1×10^6 RETs per specimen in 15 min.

Micronucleus Assay, Cell Staining, and Data Acquisition

Determinations of the frequency of MN-RET were performed using blood specimens collected on days 4 and 29 with a FACSCalibur flow cytometer providing 488-nm excitation. The necessary reagents and instructions for use were from *In Vivo* Rat MicroFlow PLUS Kits and are described in detail elsewhere (Dertinger *et al*., 2004; Torous *et al*., 2003). Kit-supplied malaria-infected erythrocytes served as biological standards and guided instrument settings on each day of analysis (Dertinger *et al*., 2000; Tometsko *et al*., 1993). The frequency of MN-RET was determined upon the acquisition of ~20,000 CD71-positive RETs per blood sample.

Calculations and Statistical Analyses

Calculations of frequency, average, SEM, and arcsine square-root transformations were performed with Excel Office X for Mac (Microsoft, Seattle, WA). All statistical tests described below were two sided and used $p < 0.05$ to indicate significance.

***Pig-a* assay.** The frequency of mutant phenotype RBCs is expressed as the number of RBC^{CD59-} per 1 million total RBCs. The frequency of mutant phenotype RETs is expressed as the number of RET^{CD59-} per 1 million total RETs. For graphical presentations, RET values for each mutagen-treated group are expressed as a percentage of the mean vehicle control value at that same time point.

Pig-a data were analyzed with SAS (v9.1) and Matlab (v2008a). The primary endpoints included the frequency of RETs among RBCs, the frequency of RET^{CD59-} among RETs, and the frequency of RBC^{CD59-} among RBCs as measured by flow cytometry. The effect of treatment on each endpoint was considered at each individual time point using the nonparametric Kruskal-Wallis test, and pairwise comparisons based on the Wilcoxon rank sum test were performed to evaluate vehicle against each of the other treatment groups.

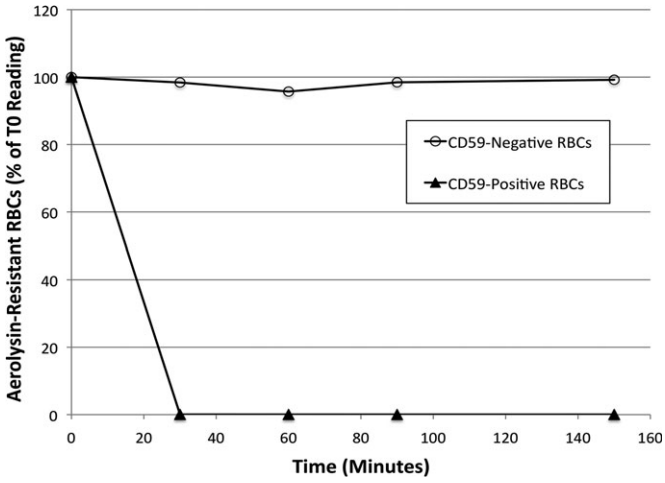

FIG. 2. Percentage of wild-type phenotype erythrocytes (CD59 positive) and mutant phenotype erythrocytes (CD59 negative) are graphed as a function of time following exposure to aerolysin. The sensitivity of CD59-positive cells is presumed to be related to their expression of GPI anchors and the insensitivity of CD59-negative erythrocytes to their lack of GPI anchors.

Additionally, in order to assess the overall significance of treatment effect across time points, the p values obtained either from the Kruskal-Wallis tests or from the Wilcoxon rank sum tests (days 15 through 56) were combined using Fisher's combination method. The associated (overall) p value was computed using a permutation approach. This was done separately for each endpoint and for RBC^{CD59-} and RET^{CD59-} jointly. Finally, mixed effects models, including a random intercept that modeled the between-experiment variability, were used to describe values of the endpoints at baseline and to compute 95% confidence intervals for the mean measurement.

Micronucleus assay. The proportion of MN-RET among RETs was transformed in Excel as follows: transformed data = asin(sqrt(proportion of MN-RET)). One-way ANOVA was used to evaluate the effect of treatment on these transformed MN-RET proportions (JMP software, v5.0 for Mac). If $p < 0.05$, each treatment group was compared to vehicle control using Dunnett's multiple comparison t-test. These analyses were performed separately for specimens obtained on day 4 and day 29.

RESULTS

Aerolysin Treatment

Results of a representative aerolysin experiment are shown in Figure 2. As aerolysin exposure time increased, fewer intact CD59-positive erythrocytes remained. These cells were presumably sensitive to aerolysin because they expressed GPI anchors. CD59-negative erythrocytes remained intact over this same time frame, presumably because they lacked GPI anchors. These data support the underlying premise of this erythrocyte-based mutation assay—that the CD59-negative phenotype is a reliable reporter of GPI anchor deficiency. The results also reinforce the appropriateness of the cell staining strategy utilized for the definitive studies described below.

Overview of Definitive Studies

As shown in Table 2, each chemical affected weight gain markedly. This was most pronounced with MNU, where animals lost nearly 9 g on average. In conjunction with information gathered during preliminary dose range finding studies and/or outward signs of toxicity noted during the definitive studies (outlined in Table 1), these data suggest that maximum tolerated doses were either reached or approached.

TABLE 2
Effect of Treatment on Weight Gain (Over 28 Days of Treatment)

Treatment (mg/kg/day)	Average weight gain (g)	Average weight gain as % control
ENU		
0	121.2	100
2.5	105.4	87
5	87.6	72
10	55.2	46
MNU		
0	92.2	100
2.5	94.6	103
5	56.8	62
10	−8.8	−10
DMBA		
0	113.2	100
2.5	122.4	108
5	88.4	78
10	57.2	51
B(*a*)P		
0	91.3	100
37.5	86.0	94
75	57.4	63
150	9.2	10
4NQO		
0	120.6	100
1.25	123.0	102
2.5	91.2	76
5	69.8	58

Data compiled from each of the 100 Wistar rat specimens collected on the day prior to treatment (20 rats per study × 5 studies) are provided in Table 3. These data demonstrate consistent low spontaneous mutant frequency values, an important requirement when such extremely rare events are being scored.

RET^{CD59-} and RBC^{CD59-} frequencies were elevated significantly following treatment with each of the five mutagenic chemicals studied ($p < 0.05$). All p values associated with these *Pig-a* assay determinations are reported in a Supplementary data file. With the exception of 4NQO, each chemical increased MN-RET frequency significantly.

N-ethyl-N-nitrosourea

Frequencies of RETs, RET^{CD59-}, RBC^{CD59-}, and MN-RET following treatment with ENU are shown in Figure 3. RET frequencies were modestly reduced by the high dose of ENU at the day 15 time point, with evidence of a rebound effect thereafter. RET^{CD59-} values were markedly increased, with

TABLE 3
Compilation of Wistar Han Pre-Dosing (day −1) Specimens, 100 Individuals

Variable	Average	SD	SEM	Upper 95% CI	Lower 95% CI
% RET	6.97	1.42	0.44	7.85	6.09
$RBC^{CD59-} \times 10^{-6}$	1.10	1.20	0.12	1.34	0.86
$RET^{CD59-} \times 10^{-6}$	1.22	1.86	0.22	1.66	0.78

Note. CI, confidence interval.

greatly elevated frequencies evident as early as day 15. RBC^{CD59-} frequencies increased more gradually, with the most substantial increases occurring between days 29 and 56. ENU also caused significant cytogenetic damage, as evidenced by increased % MN-RET values.

N-methyl-N-nitrosourea

Frequencies of RETs, RET^{CD59-}, RBC^{CD59-}, and MN-RET following treatment with MNU are shown in Figure 4. RET frequencies were modestly reduced by the high dose of MNU at the day 15 time point, with evidence of a rebound effect thereafter. RET^{CD59-} values were elevated between days 15 and 56, with the highest values tending to occur on day 29. As with ENU treatment, the most substantial MNU-induced RBC^{CD59-} responses occurred between days 29 and 56. MNU induced robust dose-related increase in micronucleus frequency on days 4 and 29. The level of MN-RET induction was markedly higher for MNU compared to ENU, even though ENU treatment generated much higher yields of mutant phenotype cells.

*7,12-Dimethyl-1,2-benz[*a*]anthracene*

Frequencies of RETs, RET^{CD59-}, RBC^{CD59-}, and MN-RET following treatment with DMBA are shown in Figure 5. RET

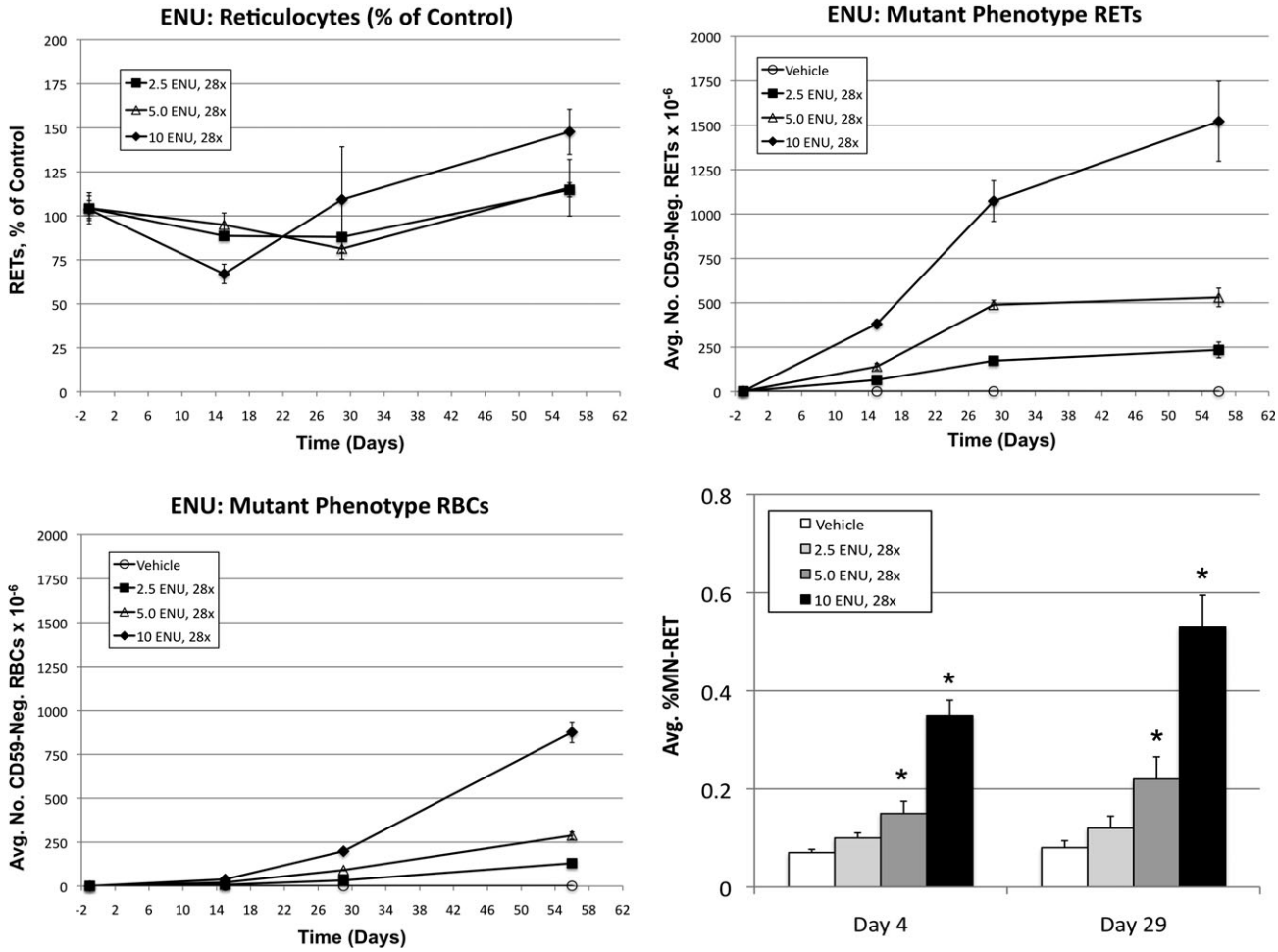

FIG. 3. Average frequencies of RETs, RET^{CD59-}, RBC^{CD59-}, and MN-RET following treatment of Wistar rats with ENU. All error bars are SEM. Upper left: Average RET frequencies as a percentage of vehicle control values as a function of time relative to treatments that occurred on days 1 through 28. Upper right: Average mutant phenotype RET frequencies as a function of time. Lower left: Average mutant phenotype erythrocyte frequencies as a function of time. Lower right: Average MN-RET frequencies at day 4 and day 29 as a function of dose. Asterisks denote statistical significance, $p < 0.05$ (Dunnett's test).

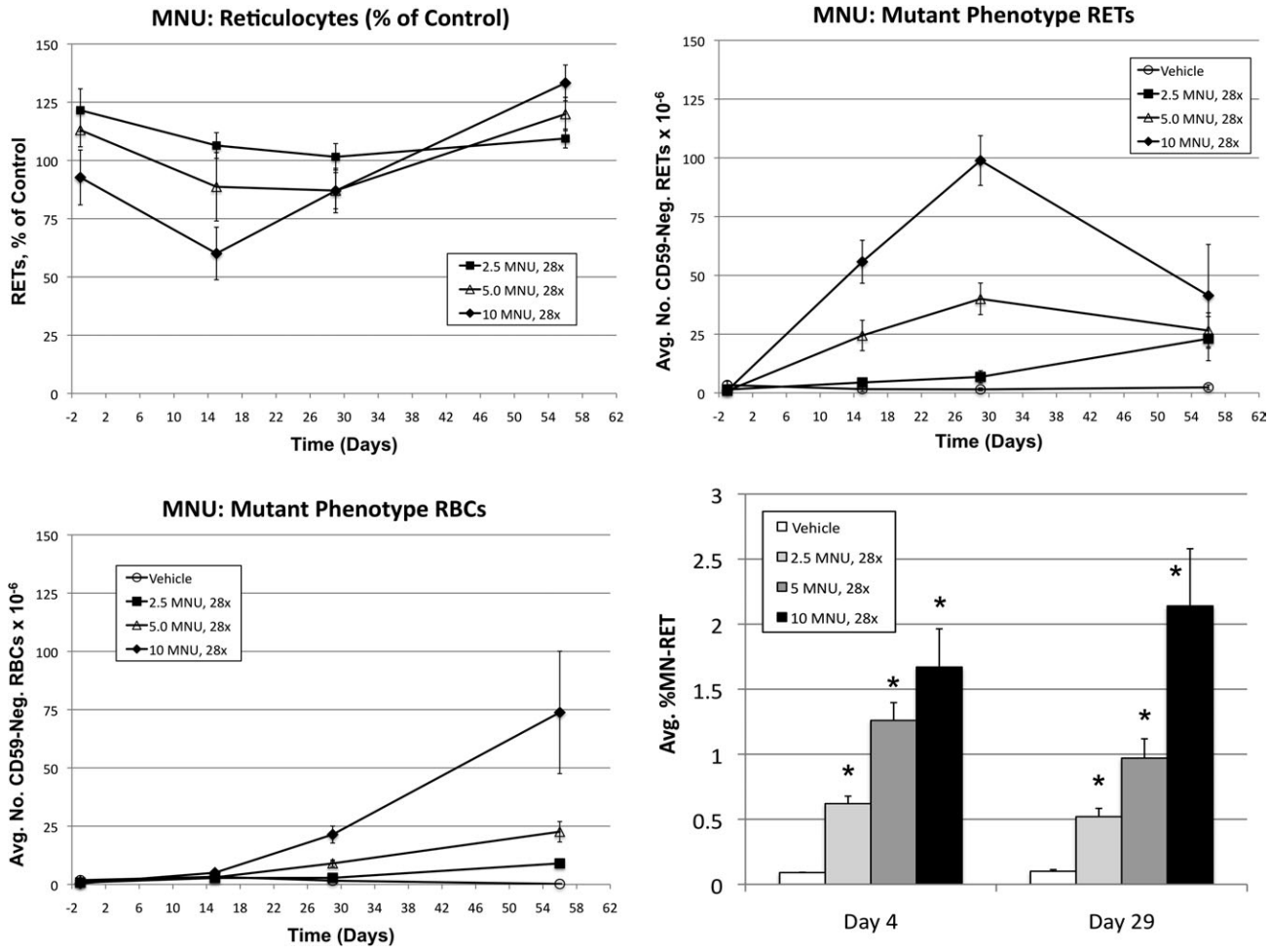

FIG. 4. Average frequencies of RETs, RET^{CD59-}, RBC^{CD59-}, and MN-RET following treatment of Wistar rats with MNU. Data are formatted as in Figure 3.

frequencies were markedly reduced by the high-dose level on days 15 and 29. Outward signs of toxicity for this group became pronounced on days 30 and 31 and stopped further investigation of these rats at that time. RET^{CD59-} values were elevated between days 15 and 56, with maximal values observed by day 29. Induced RET^{CD59-} values for the low- and mid-dose groups remained stable until the day 56 time point. Elevated RBC^{CD59-} frequencies were evident on day 29, reaching maximal values on day 56. Mean MN-RET frequencies were elevated in the high-dose group on days 4 and 29, with a more robust increase observed at the later time point.

4-Nitroquinoline-1-oxide

Frequencies of RETs, RET^{CD59-}, RBC^{CD59-}, and MN-RET following treatment with 4NQO are shown in Figure 6. Whereas treatment markedly affected weight gain, RET frequencies were not affected by 4NQO. One animal in the high-dose group was severely moribund on day 30; therefore, the group size was reduced to four thereafter. The high-dose treatment significantly increased RET^{CD59-} values on days 15 through 56. While the mid-dose group consistently exhibited modestly higher RET^{CD59-} frequencies compared to control, the effect did not reach statistical significance. 4NQO increased RBC^{CD59-} frequencies slightly, an effect that was also restricted to the high-dose group. Note that data for one high-dose animal, Q14, were not graphed at day 56 or considered in the statistical analyses at that time point. This is because the Q14 sample at day 56 exhibited extremely discrepant RET^{CD59-} and RBC^{CD59-} values (e.g., $RET^{CD59-} = 1587 \times 10^{-6}$ in the case of Q14 vs. 16.6×10^{-6} for the remaining animals in this group). The most likely explanation for this result at this time is clonal expansion of an early progenitor/stem cell. Interestingly, even though *Pig-a* mutation was evident in the erythroid lineage, no significant effect on MN-RET frequency was observed for 4NQO.

*Benzo(*a*)pyrene*

Frequencies of RETs, RET^{CD59-}, RBC^{CD59-}, and MN-RET following treatment with B(*a*)P are shown in Figure 7. RET

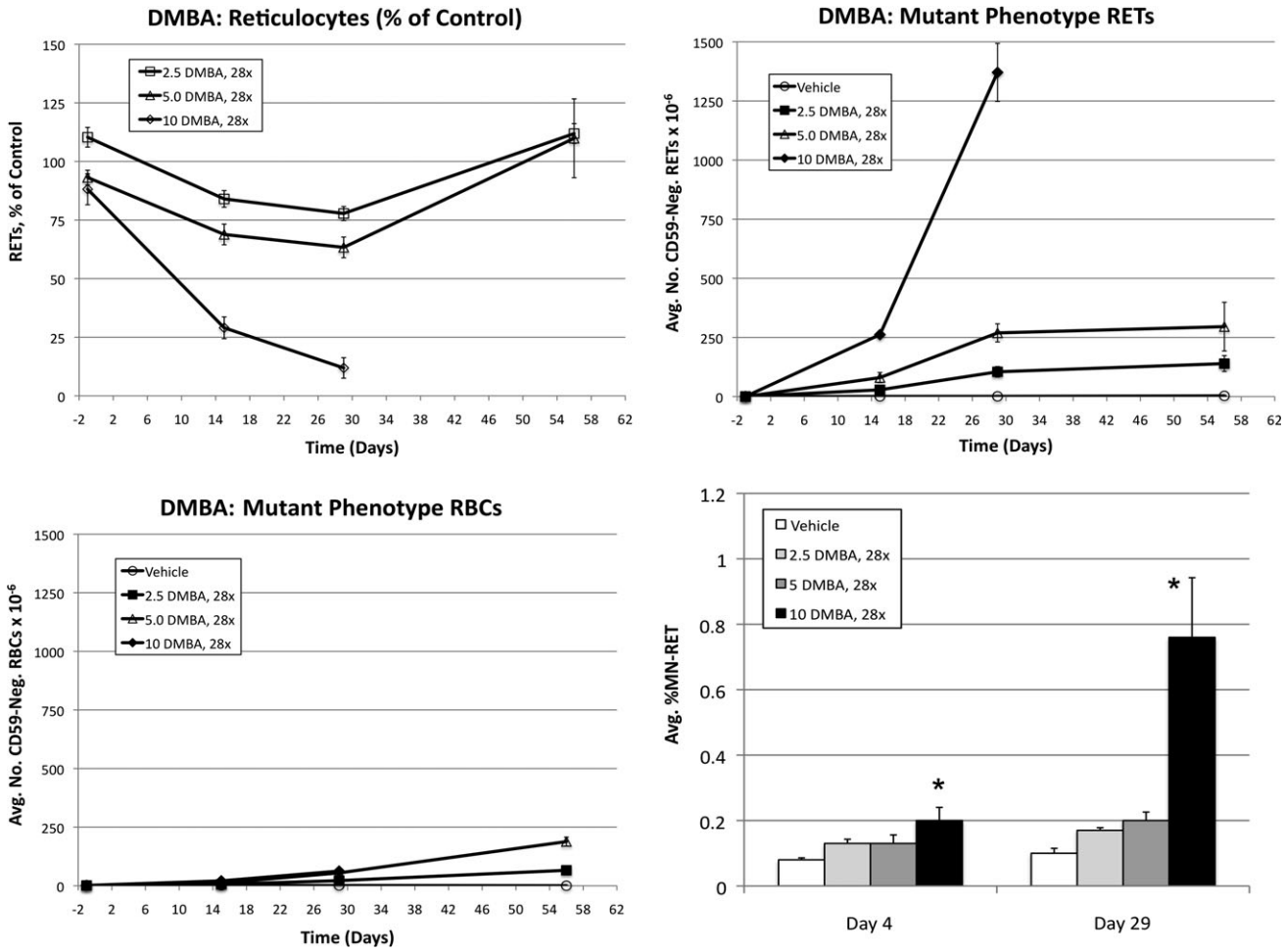

FIG. 5. Average frequencies of RETs, RET^{CD59-}, RBC^{CD59-}, and MN-RET following treatment of Wistar rats with DMBA. Data are formatted as in Figure 3.

frequencies were elevated in exposed animals, especially in high-dose animals on day 29. It is not clear at this time how temporary stimulation of erythropoiesis might affect the yield of mutant phenotype cells (RET frequencies were back to control levels on day 56). RET^{CD59-} values were elevated between days 15 and 56. While the greatest mean RET^{CD59-} value for the high-dose group was exhibited on day 56, the frequency was only slightly lower at day 29. As with the other agents, RBC^{CD59-} responses continued to rise between days 29 and 56. B(*a*)P caused dose-related increases in MN-RET on days 4 and 29.

Acute Versus Protracted Dosing: Pig-a

RET^{CD59-} frequencies resulting from 28 days or 3 days of treatment with similar total doses of ENU are presented in Figure 8. The data for the 3-day treatments are from a previous study in our laboratory that also utilized male Wistar rats (same animal supplier, age at time of treatment, sample handling protocols, etc.) (Phonethepswath *et al*., 2010). Given how closely the maximal RET^{CD59-} values compare across these acute and highly fractionated administration schedules, these data suggest that mutant phenotype cells can accumulate in a nearly additive fashion with repeat dosing, at least in the case of some chemicals like ENU.

Figure 9 shows MNU-induced RET^{CD59-} frequencies obtained in the current 28-day study along with values derived from a previous study from our laboratory that used a 3-day treatment schedule (same animal supplier, age at time of treatment, sample handling protocols, etc.) (Phonethepswath *et al*., 2010). Unlike ENU, MNU was not additive throughout the dose range examined, as fractionation of 140 and even 280 mg/kg did not approach RET^{CD59-} frequencies induced by 90 mg/kg delivered over 3 days.

DISCUSSION

Each of the five mutagenic agents studied herein increased the frequency of GPI anchor–deficient erythroid cells. Both the

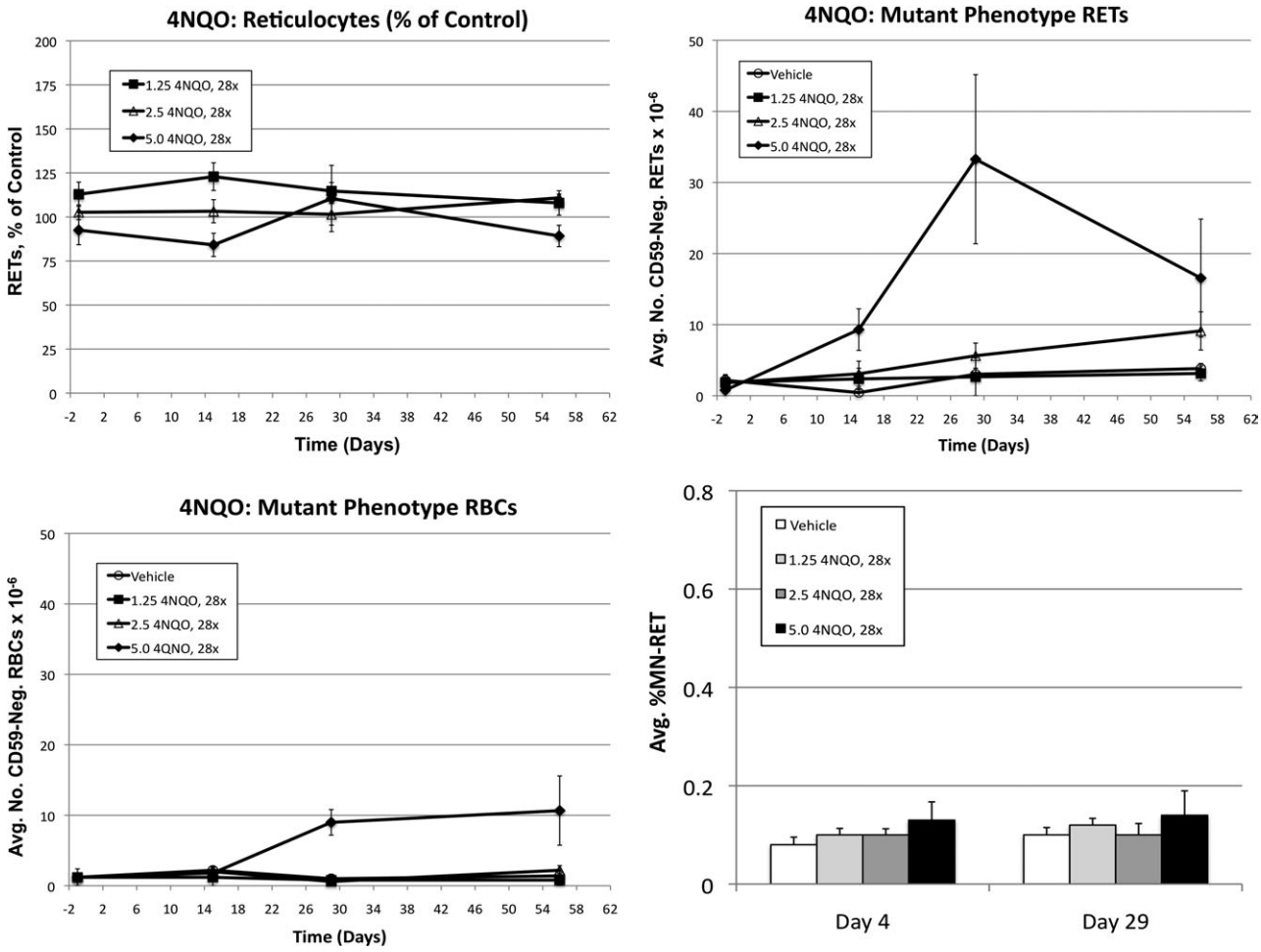

FIG. 6. Average frequencies of RETs, RET^{CD59-}, RBC^{CD59-}, and MN-RET following treatment of Wistar rats with 4NQO. Data are formatted as in Figure 3.

total RBC population and the RET subpopulation exhibited increased mutant phenotype cell frequencies, especially at the days 29 and 56 time points. However, in the standard conduct of a 28-day study, the majority of animals are not available past day 29. For this reason, the RET cohort is the appropriate cell population in which to monitor the mutant cell phenotype, as RET^{CD59-} responses are maximal or nearly so by day 29. RBC^{CD59-} responses require a significantly longer manifestation time.

The persistence of GPI anchor–deficient hematopoietic cells reported here and elsewhere (Bryce *et al*., 2008; Miura *et al*., 2009) suggests that *Pig-a* mutation is a neutral or nearly neutral event, meaning the affected cells are not highly selected for or against. Neutrality predicts that mutant cells should accumulate with repeat dosing, a desirable characteristic of transgenic rodent models, but not of most other *in vivo* genotoxicity endpoints (Heddle *et al*., 1995). Miura *et al*. (2009) demonstrated accumulation of ENU-induced *Pig-a* mutant cells with repeat dosing, and the acute versus highly fractionated ENU data presented herein support that finding. However, it is apparent that additivity of *Pig-a* mutant yield is agent specific and does not always occur throughout the range of doses that are effective at inducing mutation. This is well illustrated by MNU. In a previous report of MNU administration over 3 days, two observations are inconsistent with additivity: the 45-mg/kg dose led to considerably less than one-half the response induced by 90 mg/kg and the frequency of RET^{CD59-} dropped dramatically between days 15 and 30 time points.

We previously speculated that the extreme persistence of ENU-induced RET^{CD59-} frequencies was due to mutation in hematopoietic stem cells (Phonethepswath *et al*., 2010), whereas the fall-off of MNU-induced RET^{CD59-} indicates targeting of committed progenitors that lack self-renewal capacity. These characteristics of the 3-day study data suggest that protracted administrations of MNU would not yield maximal mutant frequencies consistent with the prediction of additivity of the individual doses. Data described herein are consistent with this reasoning, as rats exposed to a total dose of 140 and even

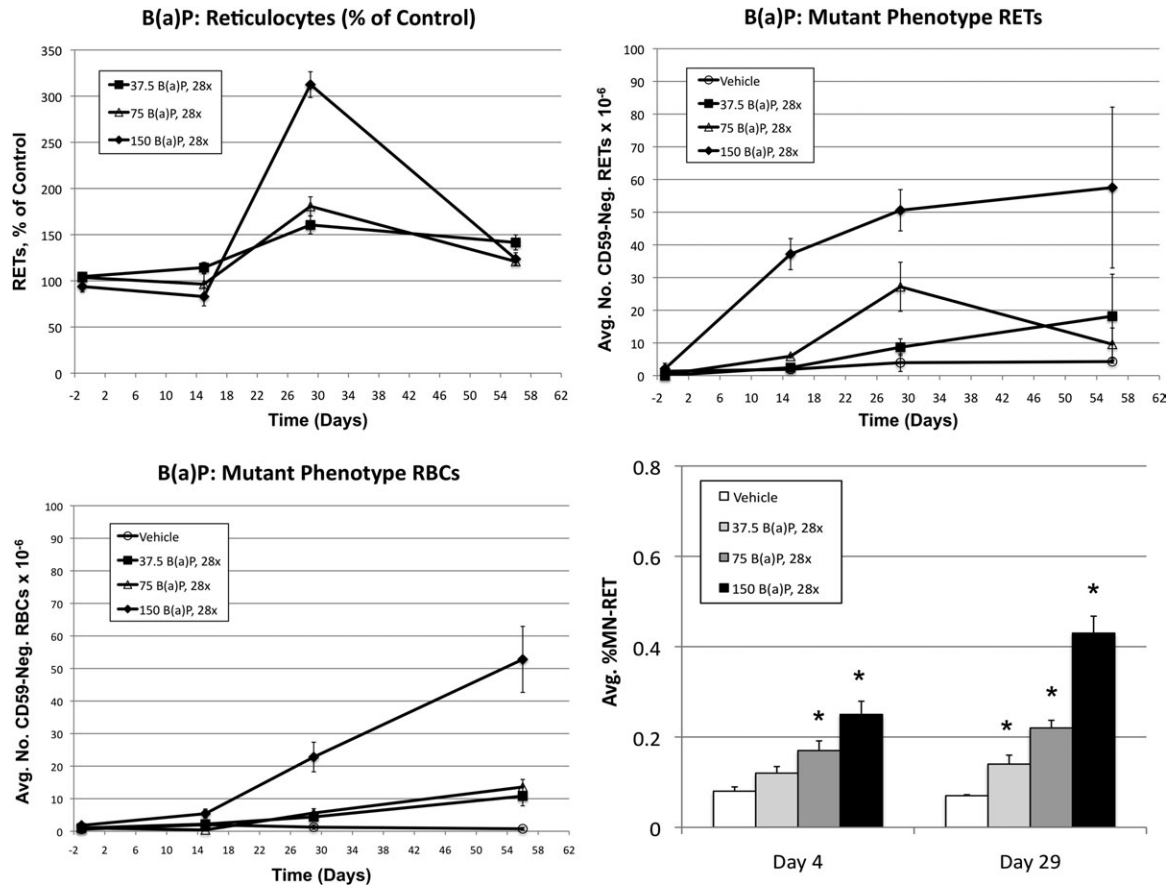

FIG. 7. Average frequencies of RETs, RET^{CD59-}, RBC^{CD59-}, and MN-RET following treatment of Wistar rats with B(*a*)P. Data are formatted as in Figure 3.

280 mg/kg over 28 days exhibited a slight response compared to the results obtained from the 3-day exposure to 90 mg/kg. One possible explanation is that DNA repair capacity can be overwhelmed by high-dose levels of MNU, whereas repair can occur more efficiently when similar exposures are fractioned over time.

Given the kinetics of MN-RET appearance and disappearance from the circulation, which are determined by the short

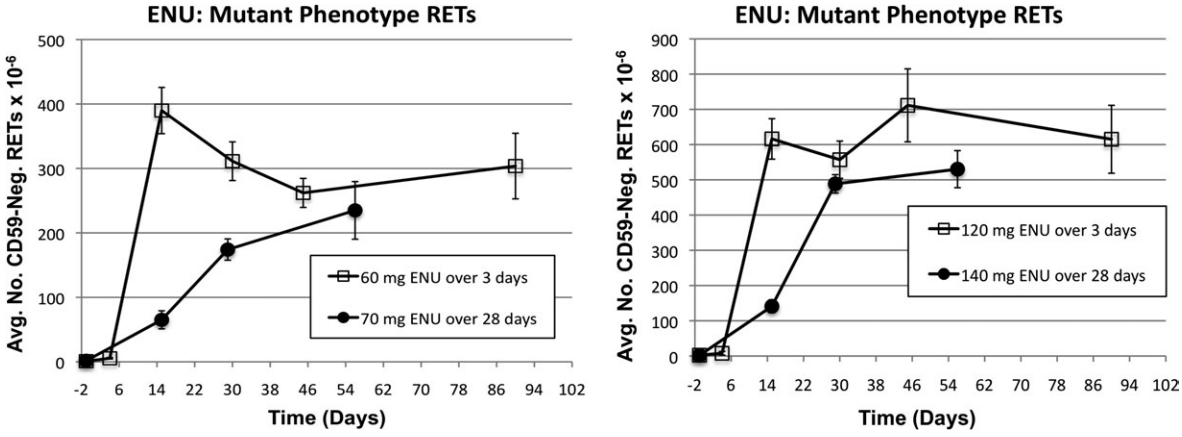

FIG. 8. Average mutant phenotype RET frequencies as a function of time after treatment with ENU for 3 versus 28 consecutive days. Error bars are SEM. The maximal RET^{CD59-} frequencies at similar total doses are close despite the very different administration schedules and suggest that ENU-induced mutant cells accumulate with repeated dosing.

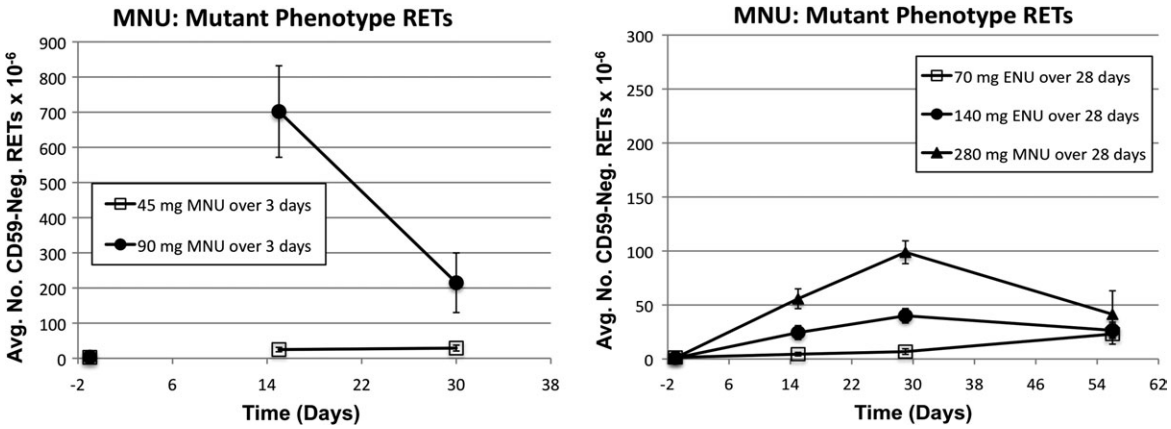

FIG. 9. Average mutant phenotype RET frequencies as a function of time after treatment with MNU for 3 versus 28 consecutive days. Error bars are SEM. These MNU data suggest that repeat dosing does not always increase the yield of mutant phenotype cells in an additive manner.

half-life of RETs and the strong selective pressure against cells that express micronuclei, the yield of MN-RET does not generally increase with repeat dosing (Hamada *et al*., 2001). Thus, it was expected that similar MN-RET frequencies would be observed on days 4 and 29. DMBA-induced MN-RET is an obvious exception in the present study. Induced metabolism and/or bioaccumulation may explain this result.

Two other observations related to the MN-RET frequencies observed in the present studies are worth noting. B(*a*)P was observed to induce MN-RET in a dose-dependent manner on days 4 and 29, a result that differs from the negative findings reported by Hamada *et al.* (2001) following 28 days of treatment. With 4NQO, high acute doses were previously shown to induce micronuclei (Phonethepswath *et al*., 2010), but the doses used herein did not significantly affect the frequency of MN-RET. The fivefold lower 4NQO dosage per day likely explains this result. Collectively, these data support the integration of the MN-RET endpoint into repeat-dosing toxicology studies, recognizing that in some cases acute exposures to higher doses may be more genotoxic.

The cytogenetic damage and mutation endpoints described herein were collected very efficiently due to the direct application of high-throughput scoring methods to small samples of peripheral blood. Processing of blood specimens and flow cytometric analyses of both endpoints generally required 1.5 technicians working approximately two full days per chemical per time point. Importantly, the expression time for mutant RET frequencies were found to be compatible with the standard conduct of 28-day toxicity studies, making it practical for the first time to integrate both mutation and cytogenetic damage measurements without the need for nonstandard rodents or harvest times or the necessity of cell culture to express mutations.

With more extensive validation of the *Pig-a* endpoint, experimental designs such as the one(s) described herein have the potential to significantly reduce the number of dedicated *in vivo* genotoxicity studies required, while at the same time improving the extent and value of available genotoxicity information. A number of laboratories are currently involved in assay validation efforts that have been designed to address the most critical data gaps that currently exist, especially (1) assessment of assay portability, (2) studies of additional mutagenic and nonmutagenic agents, (3) determination of consensus statistical approaches for analyzing *Pig-a* data, (4) DNA sequencing in order to firmly establish the link between GPI anchor deficiency with bona fide *Pig-a* mutation, (5) evaluation of the erythrocyte assay's cross-species potential, and (6) determination of whether the GPI anchor–deficient phenotype can be used to study mutation in nonerythroid cells, e.g., primary hepatocytes.

SUPPLEMENTARY DATA

Supplementary data are available online at http://toxsci.oxfordjournals.org/.

FUNDING

National Institutes of Health/National Institute of Environmental Health Sciences (grant no. R44ES015940).

ACKNOWLEDGMENTS

The contents are the sole responsibility of the authors and do not necessarily represent the official views of the institutions with which they are affiliated or of the National Institute of Environmental Health Sciences (NIEHS). The authors would like to thank Ronald Fiedler, Laura Custer, George Douglas, and members of the Health and Environmental Sciences Institute (HESI) Pig-a Validation Group—James Kim, Robert Heflich, Veronique Thybaud, Bhaskar Gollapudi, Vasily

Dobrovolsky, Jan van Benthem, and Jennifer Sasaki—who shared valuable advice, especially in regard to choice of chemicals and dose levels. Disclosure: several of the authors are employed by Litron Laboratories, a company that sells MicroFlow Kits that can be used to score rodent MN-RET frequencies as described herein; J. MacGregor, J. Palis, and O. Hyrien serve as consultants to Litron Laboratories under the NIEHS-funded grant; Litron Laboratories has filed patent applications that relate to mutation measurements based on the GPI anchor deficiency phenotype as a means to quantify *Pig-a* gene mutation frequency.

REFERENCES

Araten, D. J., Nafa, K., Pakdeesuwan, K., and Luzzatto, L. (1999). Clonal populations of hematopoietic cells with paroxysmal nocturnal hemoglobinuria genotype and phenotype are present in normal individuals. *Proc. Natl. Acad. Sci. U.S.A.* **96,** 5209–5214.

Blakey, D., Galloway, S. M., Kirkland, D. J., and MacGregor, J. T. (2008). Regulatory aspects of genotoxicity testing: from hazard identification to risk assessment. *Mutat. Res.* **657,** 84–90.

Bryce, S. M., Bemis, J. C., and Dertinger, S. D. (2008). *In vivo* mutation assay based on the endogenous *Pig-a* locus. *Environ. Mol. Mutagen.* **49,** 256–264.

Dertinger, S. D., Camphausen, K., MacGregor, J. T., Bishop, M. E., Torous, D. T., Avlasevich, S., Cairns, S., Tometsko, C. R., Menard, C., Muanza, T., *et al.* (2004). Three-color labeling method for flow cytometric measurement of cytogenetic damage in rodent and human blood. *Environ. Mol. Mutagen.* **44,** 427–435.

Dertinger, S. D., Torous, D. K., Hall, N. E., Tometsko, C. R., and Gasiewicz, T. A. (2000). Malaria-infected erythrocytes serve as biological standards to ensure reliable and consistent scoring of micronucleated erythrocytes by flow cytometry. *Mutat. Res.* **464,** 195–200.

Diep, D. B., Nelson, K. L., Raja, S. M., Pleshak, E. N., and Buckley, J. T. (1998). Glycosylphosphatidylinositol anchors of membrane glycoproteins are binding determinants for the channel-forming toxin aerolysin. *J. Biol. Chem.* **273,** 2355–2360.

Dobrovolsky, V. N., Boctor, S. Y., Twaddle, N. C., Doerge, D. R., Bishop, M. E., Manjanatha, M. G., Kimoto, T., Miura, D., Heflich, R. H., and Ferguson, S. A. (2010). Flow cytometric detection of Pig-A mutant red blood cells using an erythroid-specific antibody: application of the method for evaluating the *in vivo* genotoxicity of methylphenidate in adolescent rats. *Environ. Mol. Mutagen.* **51,** 138–145.

Hamada, S., Sutou, S., Morita, T., Wakata, A., Asanami, S., Hosoya, S., Ozawa, S., Kondo, K., Nakajima, M., Shimada, H., *et al.* (2001). Evaluation of the rodent micronucleus assay by a 28-day treatment protocol: summary of the 13th collaborative study by the colloborative study group for the micronucleus test (CSGMT)/environmental mutagen society of Japan (JEMS)—mammalian mutagenicity study group (MMS). *Environ. Mol. Mutagen* **37,** 93–110.

Heddle, J. A., Shaver-Walker, P., Tao, K. S., and Zhang, X. B. (1995). Treatment protocols for transgenic mutation assays *in vivo*. *Mutagenesis* **10,** 467–470.

International Conference on Harmonization. (2008). *Guidance on Genotoxicity Testing and Data Interpretation for Pharmaceuticals Intended for Human Use S2(R1) (2008, draft).* Available at: http://www.ich.org/LOB/media/MEDIA4474.pdf.

Krishna, G., Urda, G., and Theiss, J. (1998). Principles and practices of integrating genotoxicity evaluation into routine toxicology studies: a pharmaceutical industry perspective. *Environ. Mol. Mutagen.* **32,** 115–120.

MacGregor, J. T., Bishop, M. E., McNamee, J. P., Hayashi, M., Asano, N., Wakata, A., Nakajima, M., Saito, J., Aidoo, A., Moore, M. M., *et al.* (2006). Flow cytometric analysis of micronuclei in peripheral blood reticulocytes: II. An efficient method of monitoring chromosomal damage in the rat. *Toxicol. Sci.* **94,** 92–107.

Miura, D., Dobrovolsky, V. N., Kasahara, Y., Katsuura, Y., and Heflich, R. H. (2008a). Development of an in vivo gene mutation assay using the endogenous *Pig-A* gene: I. Flow cytometric detection of CD59-negative peripheral red blood cells and CD48-negative spleen T-cells from the rat. *Environ. Mol. Mutagen.* **49,** 614–621.

Miura, D., Dobrovolsky, V. N., Kimoto, T., Kasahara, Y., and Heflich, R. H. (2009). Accumulation and persistence of *Pig-A* mutant peripheral red blood cells following treatment of rats with single and split doses of N-ethyl-N-nitrosourea. *Mutat. Res.* **677,** 86–92.

Miura, D., Dobrovolsky, V. N., Mittelstaedt, R. A., Kasahara, Y., Katsuura, Y., and Heflich, R. H. (2008b). Development of an in vivo gene mutation assay using the endogenous *Pig-A* gene: II. Selection of Pig-A mutant rat spleen T-cells with proaerolysin and sequencing *Pig-A* cDNA from the mutants. *Environ. Mol. Mutagen.* **49,** 622–630.

Pfuhler, S., Kirkland, D., Kasper, P., Hayashi, M., Vanparys, P., Carmichael, P., Dertinger, S., Eastmond, D., Elhajouji, A., Krul, C., *et al.* (2009). Reduction of use of animals in regulatory genotoxicity testing: identification and implementation opportunities—report from an ECVAM workshop. *Mutat. Res.* **680,** 31–42.

Phonethepswath, S., Bryce, S. M., Bemis, J. C., and Dertinger, S. D. (2008). Erythrocyte-based *Pig-a* gene mutation assay: demonstration of cross-species potential. *Mutat. Res.* **657,** 122–126.

Phonethepswath, S., Franklin, D., Torous, D. K., Bryce, S. M., Bemis, J. C., Raja, S., Avlasevich, S., Weller, P., Hyrien, O., Palis, J., *et al.* (2010). *Pig-a* mutation: kinetics in rat erythrocytes following exposure to five prototypical mutagens. *Toxicol. Sci.* **114,** 59–70.

Tometsko, A. M., Torous, D. K., and Dertinger, S. D. (1993). Analysis of micronucleated cells by flow cytometry. 1. Achieving high resolution with a malaria model. *Mutat. Res.* **292,** 129–135.

Torous, D. K., Hall, N. E., Murante, F. G., Gleason, S. E., Tometsko, C. R., and Dertinger, S. D. (2003). Comparative scoring of micronucleated reticulocytes in rat peripheral blood by flow cytometry and microscopy. *Toxicol. Sci.* **74,** 309–314.

U.S. Food and Drug Administration, Center for Drug Evaluation and Research. (2006). *Guidance for Industry, Investigators, and Reviewers.* Available at: http://www.fda.gov/downloads/Drugs/GuidanceComplianceRegulatoryInformation/Guidances/ucm078933.pdf.